J|A|C|S
ARTICLES
Published on Web 07/26/2002

Ammoniated Alkali Fullerides $(ND_3)_xNaA_2C_{60}$: Ammonia Specific Effects and Superconductivity

Serena Margadonna,*,† Efstathios Aslanis,‡ and Kosmas Prassides*,‡

Contribution from the Department of Chemistry, University of Cambridge, Cambridge CB2 1EW, U.K. and the School of Chemistry, Physics and Environmental Science, University of Sussex, Brighton BN1 9QJ, U.K.

Received May 3, 2002

Abstract: The crystal structure of the superconducting $(ND_3)_xNaA_2C_{60}$ ($0.7 \leq x \leq 1$, A= K, Rb) fullerides (T_c= 6−15 K) has been studied by synchrotron X-ray and neutron powder diffraction. It is face-centered cubic (fcc) to low temperatures with Na^+-ND_3 pairs residing in the octahedral interstices. These are disordered over the corners of two "interpenetrating" cubes with the Na^+ ions and the N atoms displaced by ∼2.0 Å and ∼0.5 Å from the center of the site and statically disordered over the corners of the inner and outer cube, respectively. Close contacts between the D atoms of the ND_3 molecules and electron rich 6:6 C−C bonds of neighboring C_{60} units provide the signature of weak N−D···π hydrogen-bonding interactions, which control the intermolecular packing in the crystal and may determine the unusual superconducting properties.

Introduction

The key experimental observation that in the cubic alkali fullerides (A_3C_{60}) the superconducting transition temperature, T_c, increases monotonically with the interfullerene separation[1] has driven most of the attempts toward the synthesis of new superconducting fulleride salts with large lattice parameters.[2,3] This effort has recently culminated in the appearance of superconductivity at 117 K in the hole-doped $C_{60}/CHBr_3$ co-intercalate in a field-effect device.[4] This well-established trend can be explained by the BCS weak coupling theory in which T_c is controlled by the density of states at the Fermi level, $N(\epsilon_F)$, which increases with increasing intermolecular separation as a direct consequence of the reduction in the width of the conduction band.

In the fcc structure of the parent superconducting fullerides A_3C_{60}, the A^+ ions occupy octahedral and tetrahedral interstices between the C_{60}^{3-} ions, implying that the maximum lattice expansion which can be achieved by using alkali metals is limited by the maximum size of the A^+ cations ($r_{max} \leq r(Cs^+)$ = 1.69 Å) used for intercalation. However, the size of the octahedral interstices is larger than the ionic radius of any alkali ion, thereby allowing possible occupation of the site by small molecular cations or clusters, which would act as structural "spacers" further expanding the fcc array. To achieve higher T_c's, it is fundamental that the spacer used to increase the interfullerene separation should not interfere with the charge transfer as superconductivity is strongly suppressed by deviations from an exactly half-filled t_{1u} band.[5,6] The obvious choice is to employ as structural spacers alkali ions solvated with neutral molecules, such as ammonia. For instance, upon ammoniation of Na_2CsC_{60}, the lattice expands and the cubic symmetry is maintained: the lattice constant increases by ∼0.39 Å and T_c increases significantly from 10.5 to 29.6 K.[7]

However, this behavior is not general, as the introduction of NH_3 in the interstitial sites of other alkali fullerides has been found to lead to diverse responses in the structural and conducting properties. For example in K_3C_{60}, introduction of one ammonia molecule in the octahedral site of the fcc structure to form $(NH_3)K_3C_{60}$ produces an anisotropic expansion of the fulleride array, inducing a symmetry reduction,[8,9] development of antiferromagnetic long-range order[10] below ∼40 K, and suppression of superconductivity at ambient pressure.[11] Ap-

* To whom correspondence should be addressed. E-mail: sm413@hermes.cam.ac.uk, K.Prassides@susx.ac.uk.
† University of Cambridge.
‡ University of Sussex.

(1) Fleming, R. M.; Ramirez, A. P.; Rosseinsky, M. J.; Murphy, D. W.; Haddon, R. C.; Zahurak, S. M.; Makhija, A. V. *Nature* **1991**, *352*, 787.
(2) Tanigaki, K.; Hirosawa, I.; Ebbesen, T. E.; Mizuki, J.; Shimakawa, Y.; Kubo, Y.; Tsai, J. S.; Kuroshima, S. *Nature* **1992**, *356*, 419.
(3) Dahlke, P.; Denning, M. S.; Henry, P. F.; Rosseinsky, M. J. *J. Am. Chem. Soc.* **2000**, *122*, 12352.
(4) Schön, J. H.; Kloc, C.; Batlogg, B. *Science* **2001**, *293*, 2432.
(5) Yildirim, T.; Barbedette, L.; Fischer, J. E.; Lin, C. L.; Robert, J.; Petit, P.; Palstra, T. T. M. *Phys. Rev. Lett.* **1996**, *77*, 167.
(6) Kosaka, M.; Tanigaki, K.; Prassides, K.; Margadonna, S.; Brown, C. M.; Lappas, A.; Fitch, A. N. *Phys. Rev. B* **1999**, *59*, R6628.
(7) Zhou, O.; Fleming, R. M.; Murphy, D. W.; Rosseinsky, M. J.; Ramirez, A. P.; van Dover, R. B.; Haddon, R. C. *Nature* **1993**, *362*, 433.
(8) Rosseinsky, M. J.; Murphy, D. W.; Fleming, R. M.; Zhou, O. *Nature* **1993**, *364*, 425. Zhou, O.; Palstra, T. T. M.; Iwasa, Y.; Fleming, R. M.; Hebard, A. F.; Sulewski, P. E. *Phys. Rev. B* **1995**, *52*, 483.
(9) Ishii, K.; Watanuki, T.; Fujiwara, A.; Suematsu, H.; Iwasa, Y.; Shimoda, H.; Mitani, T.; Nakao, H.; Fujii, Y.; Murakami, Y.; Kawada, H. *Phys. Rev. B* **1999**, *59*, 3956. Margadonna, S.; Prassides, K.; Shimoda, H.; Takenobu, T.; Iwasa, Y. *Phys. Rev. B* **2001**, *64*, 132414.
(10) Prassides, K.; Margadonna, S.; Arcon, D.; Lappas, A.; Shimoda, H.; Iwasa, Y. *J. Am. Chem. Soc.* **1999**, *121*, 11227. Tou, H.; Maniwa, Y.; Iwasa, Y.; Shimoda, H.; Mitani, T. *Phys. Rev. B* **2000**, *62*, R775. Simon, F.; Janossy, A.; Muranyi, F.; Feher, T.; Shimoda, H.; Iwasa, Y.; Forro, L. *Phys. Rev. B* **2000**, *61*, R3826.
(11) Iwasa, Y.; Shimoda, H.; Palstra, T. T. M.; Maniwa, Y.; Zhou, O.; Mitani, T. *Phys. Rev. B* **1996**, *53*, R8836. Allen, K. M.; Heyes, S. J.; Rosseinsky, M. J. *J. Mater. Chem.* **1996**, *6*, 1445.

10.1021/ja026775k CCC: $22.00

plication of a pressure (>1 GPa) leads to recovery of superconductivity with $T_c = 28$ K.[12] The proximity of $(NH_3)K_3C_{60}$ to a metal−insulator transition can be ascribed to the combined effects of crystal symmetry lowering and increased interfullerene separation. Similar behavior is exhibited by the series of monoammoniated alkali fullerides, $(NH_3)K_{3-x}Rb_xC_{60}$ ($0 \leq x \leq 3$), which are isostructural with $(NH_3)K_3C_{60}$ with Néel temperatures, T_N, showing a systematic change with interfullerene spacing.[13] These results suggest that the symmetry reduction upon ammoniation from fcc to orthorhombic plays a crucial role for the suppression of superconductivity and that the triple degeneracy of the t_{1u} molecular orbital is fundamental for maintaining the metallic state.

In this picture, quite puzzling are the properties displayed by the series of ammoniated fullerides, $(NH_3)_xNaA_2C_{60}$ ($0.5 \leq x \leq 1$, A = K, Rb).[14] In these systems, the fcc structure is maintained with the ammonia coordinated to the sodium ions and the Na^+-NH_3 pairs residing in the octahedral sites. However, the observed T_c's are dramatically lower than expected from simple considerations of the separation between fulleride units and, in addition, they decrease with increasing lattice constant, showing a trend which is completely different from the conventional one. The suppression of superconductivity was attributed to the presence of Na^+ ions displaced by ~0.5 Å from the center of the octahedral sites which leads to a noncubic local potential on the C_{60}^{3-} ions and could lift the triple degeneracy of the t_{1u} LUMO.

In an attempt to obtain a better understanding of the structure of these ammoniated fullerides and its implications for superconductivity, we have undertaken a systematic combined high-resolution synchrotron X-ray and neutron diffraction study of the series of perdeuterated superconductors, $(ND_3)_xNaKRbC_{60}$ and $(ND_3)_xNaRb_2C_{60}$ ($0.7 < x < 1$). By combining the complementary advantages of the two diffraction techniques, we have been able to monitor in detail the structural properties as a function of ND_3 content, x, and to search for factors which could explain the observed nonrigid band behavior by modifying the electronic state of the C_{60} units. We found that a network of weak $N-D\cdots\pi$ hydrogen bonds is formed between the ammonia molecules and selected 6:6 carbon bonds of C_{60} and that the displacement of the Na^+ ions from the center of the octahedral interstices is much larger than reported before[14] (in excess of 2.0 Å).

Experimental Details

Gram quantities of $(ND_3)_xNaKRbC_{60}$ and $(ND_3)_xNaRb_2C_{60}$ samples were synthesized by reacting stoichiometric amounts of alkali metals (Na, K, Rb) and C_{60} powder in liquid ND_3. The alkali metal and C_{60} reaction mixture was introduced in a Pyrex glass tube apparatus and cooled in a dry ice/acetone slush bath kept at −65 °C. Predried anhydrous liquid ND_3 was condensed into the tube, which was shaken for 30 min until all solid material was completely dissolved into liquid ND_3. Following slow evaporation of ND_3, the resulting powders were dried at ambient temperature under dynamic vacuum (10^{-2} Torr) for 12 h. In addition to these samples (KRb(1) and Rb2(1)), two more types of $(ND_3)_xNaKRbC_{60}$ and $(ND_3)_xNaRb_2C_{60}$ compositions were prepared by further drying and annealing at elevated temperatures. KRb(2) and Rb2(2) were additionally dried for 1 h at 110 °C under a dynamic vacuum of 10^{-4} Torr and then were sealed under 500 Torr of He gas and were annealed at 100 °C for 1 day. KRb(3) and Rb2(3) were synthesized by a similar protocol but were dried and annealed at temperatures of 130 °C and 120 °C, respectively. Phase purity was confirmed by X-ray powder diffraction with a Siemens D5000 diffractometer. SQUID measurements under zero-field cooling (ZFC) and field cooling (FC) protocols were performed at 10 Oe on samples (~25−100 mg) sealed in quartz tubes in the temperature range 1.8−30 K with a Quantum Design SQUID magnetometer.

High-resolution synchrotron X-ray diffraction measurements were performed on powdered samples sealed in 0.5-mm diameter glass capillaries. Data on the KRb(1), KRb(2), KRb(3), Rb2(2), and Rb2(3) samples were collected at 10 K in continuous scanning mode using nine Ge(111) analyzer crystals on the BM16 beamline at the European Synchrotron Radiation Facility (ESRF, Grenoble, France) with $\lambda = 0.80002$ Å for KRb(1) and 0.85041 Å for KRb(2), KRb(3), Rb2(2), and Rb2(3). The data were rebinned in the 2θ range 4− 63° to a step of 0.01°. The Rb2(1) sample was measured at 16 K on the BL0B2 beamline at Spring-8 (Japan) with an image plate detector ($\lambda = 0.88095$ Å). One-dimensional diffraction patterns were obtained by integrating around the rings using local software.

Neutron diffraction data were collected on all samples except Rb2(3). The experiments were undertaken with the high-flux high-resolution diffractometer D2b ($\lambda = 1.5944$ Å) at the Institut Laue Langevin (ILL, Grenoble, France). The samples (~0.9−1.0 g), from the same batch used for synchrotron X-ray diffraction measurements, were loaded in cylindrical vanadium cans (diameter = 5 mm) sealed with indium wire and then placed in a standard ILL "orange" liquid helium cryostat. The instrument was operated in its high-resolution mode and the data were collected in the angular range, $2\theta = 0-164.5°$ in steps of 0.05°. Full diffraction profiles were measured with counting times of 10 h at 10 K. The raw data were merged and normalized to standard vanadium runs using local ILL programs. Analysis of the diffraction data for all compounds was performed with the GSAS suite of Rietveld analysis programs.[15]

Results

Magnetization Measurements. Figure 1 shows the temperature dependence of the ZFC susceptibility of all six samples measured at a field of 10 Oe. Diamagnetic shielding is evident for all samples at low temperatures, signaling the onset of bulk superconductivity (at temperatures between 6 and 15 K, obtained by the intersection of line extrapolations made both below and above T_c), which varies with annealing times and the nature of the alkali metal ions.

Structural Analysis of the $(ND_3)_xNaKRbC_{60}$ Series. The synchrotron X-ray and neutron powder diffraction profiles collected at 10 K on the KRb(1) sample did not show any reflections violating face-centered cubic (fcc) extinction rules. Thus, the starting structural model used in the Rietveld refinement was based on the room temperature fcc structure (space group $Fm\bar{3}m$) reported by Shimoda et al.[14] for the parent compounds $(NH_3)_xNaK_2C_{60}$ and $(NH_3)_xNaRb_2C_{60}$ implying the absence of any structural transition with decreasing temperature. The combined refinement of the two data sets was initiated with the ideal stoichiometric composition: the (ND_3) content x was set equal to 1, the tetrahedral sites were fully occupied by K

(12) Zhou, O.; Palstra, T. T. M.; Iwasa, Y.; Fleming, R. M.; Hebard, A. F.; Sulewski, P. E. *Phys. Rev. B* **1995**, *52*, 483. Margadonna, S.; Prassides, K.; Shimoda, H.; Iwasa, Y.; Mézouar, M. *Europhys. Lett.* **2001**, *56*, 61.
(13) Takenobu, T.; Muro, T.; Iwasa, Y.; Mitani, T. *Phys. Rev. Lett.* **2000**, *85*, 381.
(14) Shimoda, H.; Iwasa, Y.; Miyamoto, Y.; Maniwa, Y.; Mitani, T. *Phys. Rev. B* **1996**, *54*, 15653. Iwasa, Y.; Shimoda, H.; Miyamoto, Y.; Mitani, T.; Maniwa, Y.; Zhou, O.; Palstra, T. T. M. *J. Phys. Chem. Solids* **1997**, *58*, 1697.
(15) Larsen, A. C.; von Dreele, R. B. GSAS software, Los Alamos National Laboratory Report No. LAUR 86-748; 1986.

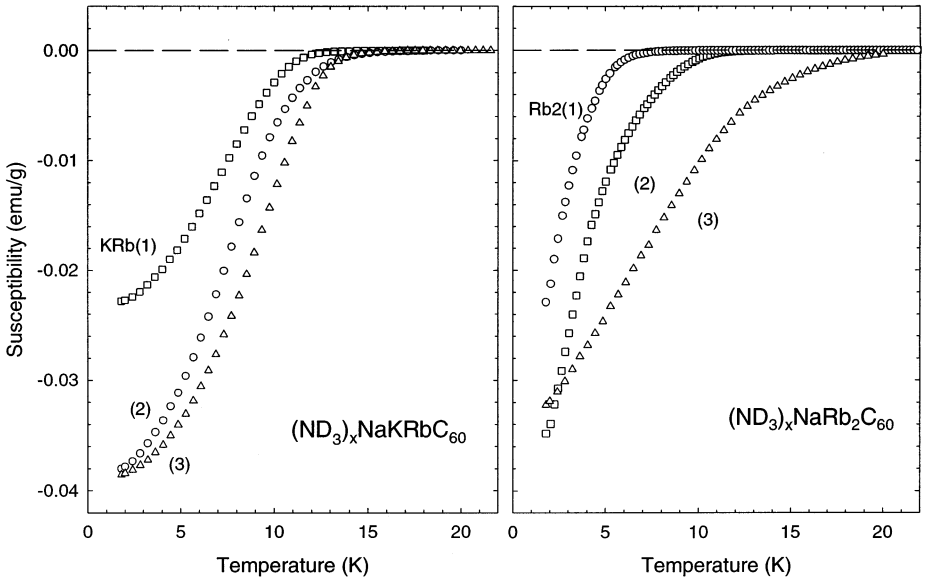

Figure 1. Temperature dependence of the magnetic susceptibility of the $(ND_3)_xNaKRbC_{60}$ and $(ND_3)_xNaRb_2C_{60}$ samples measured under ZFC conditions in a field of 10 Oe. Compositions with different x are labeled as described in the text.

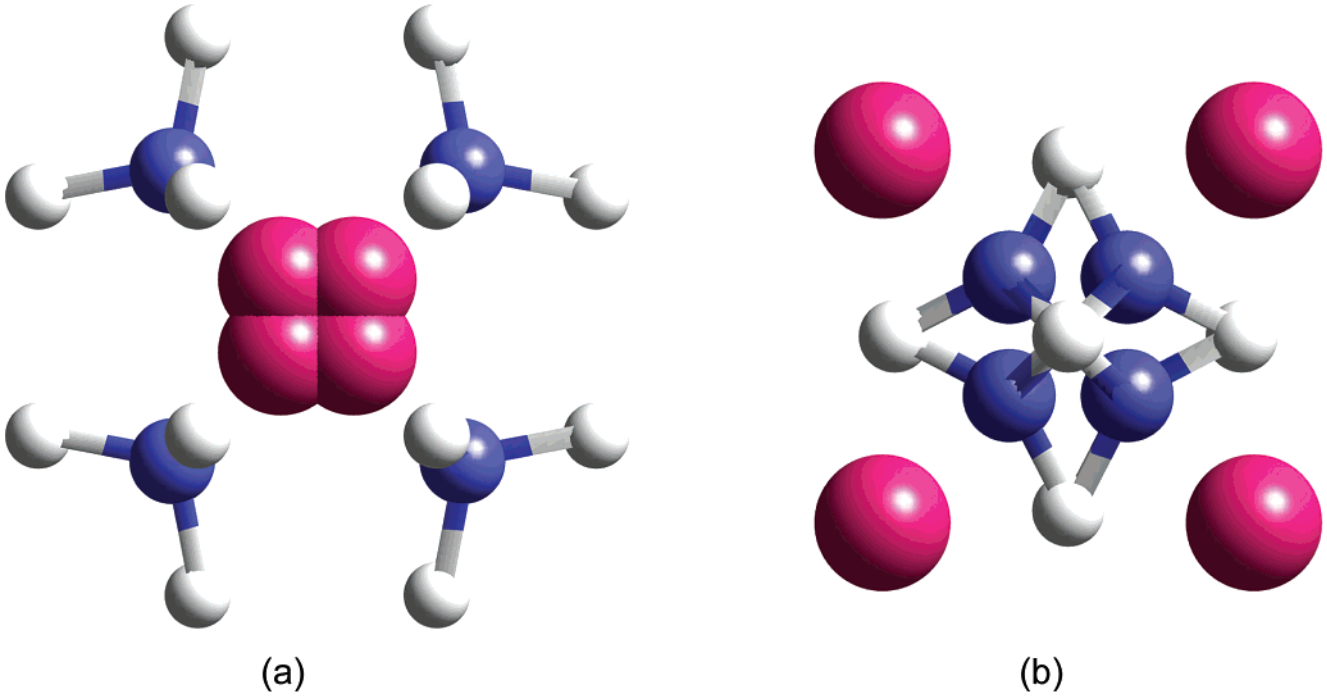

Figure 2. (a) Structural model proposed in ref 14 of the disordered $Na(ND_3)$ units which are randomly aligned along eight equivalent (111) orientations and reside in the octahedral holes of the face-centered cubic structure of $(ND_3)_xNaKRbC_{60}$ and $(ND_3)_xNaRb_2C_{60}$. (b) Same as in (a) but with the Na and ND_3 positions at the corners of the two interpenetrating cubes interchanged.

and Rb cations, while the Na−ND_3 pairs were placed in the larger octahedral hole. The Na^+ ions were displaced from the center of the octahedral site at the 32*f* (*x*,*x*,*x*; $x \approx 0.484$) positions and were disordered over the corners of a cube, centered at the ($^1/_2$,$^1/_2$,$^1/_2$) site. In the original model,[14] the NH_3 molecules were approximated by isoelectronic Ne atoms located in 32*f* (*y*,*y*,*y*; $y \approx 0.583$) off-centered positions, which also described a cube centered at ($^1/_2$,$^1/_2$,$^1/_2$).

In the present case, the ND_3 molecules are introduced explicitly with the N atoms in the original X-ray 32*f* Ne positions and the D atoms placed in 96*k* (*x*,*x*,*z*; $x \approx 0.560$, $z \approx 0.641$) positions which describe the standard geometry of the ND_3 molecule (N−D distance ≈ 1.0 Å and D−N−D angle ≈ 109°). The model comprises two "interpenetrating" cubes centered at ($^1/_2$,$^1/_2$,$^1/_2$) (Figure 2a) with the Na^+ ions and the N atoms statically disordered over the corners of the inner and outer cube, respectively. Every Na^+ ion coordinates along a body diagonal with a N atom at the opposite corner of the external cube with a Na−N distance of ca. 2.5 Å. The C_{60}^{3-} units, placed in the 4*a* position, are merohedrally disordered and are oriented with their C_2 axes parallel to the unit cell edges.

However, the combined Rietveld refinement did not proceed smoothly within this model. While the agreement of the calculated profile with the measured synchrotron X-ray data was

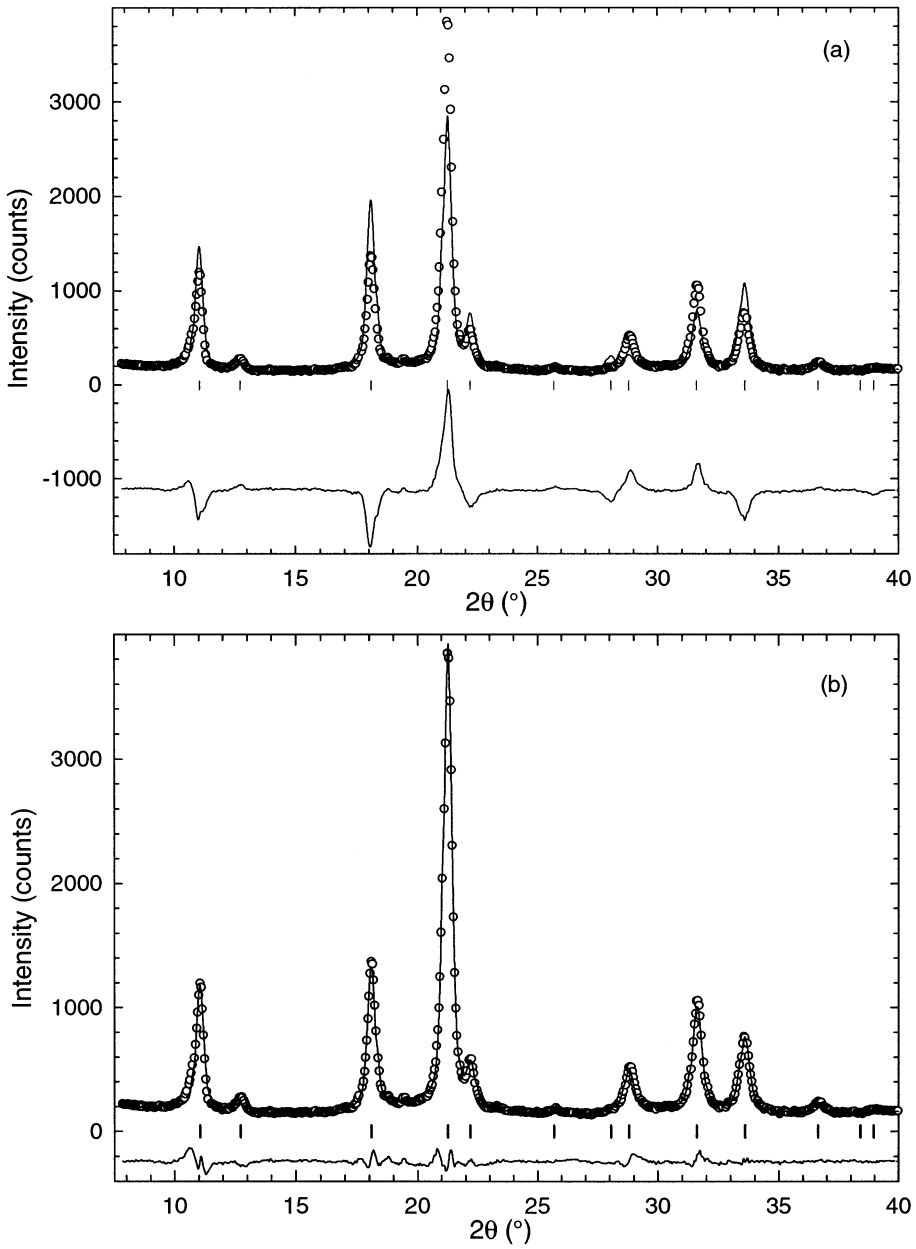

Figure 3. Observed (o) and calculated (solid line) powder neutron ($\lambda = 1.5944$ Å) diffraction profiles for $(ND_3)_{0.97}NaKRbC_{60}$ (KRb(1)) at 10 K in the range 7.5°−40° using the structural model of Figure 2a (a) and Figure 2b (b) for the disordered $Na(ND_3)$ units. In each case, the lower solid line shows the difference profile and the tic marks show the reflection positions.

satisfactory (R_{wp}= 5.8%), the neutron diffraction profile was very poorly described (R_{wp}= 16.0%), especially in the low 2θ region. The severe disagreement between calculated and observed intensity of the strong neutron peaks (Figure 3a) indicates the possibility of either a nonstoichiometric composition with cation disorder or a misplacement of the Na−ND_3 pair in the employed model, especially as it incorporated unphysically small D−C contacts (∼1.88 Å). The former hypothesis was explored by disordering the Rb ions over the octahedral and tetrahedral sites with fractional occupancies x and $(1 - x)$, respectively. By following the previous X-ray results,[14] the ammonia content was allowed to be smaller than 1 with the remaining $(1 - x)$ Na^+ ions placed in the tetrahedral hole. Despite the modified cation arrangement, the quality of the refinement of the neutron data remained completely unsatisfactory (R_{wp}= 15.5%), implying that the Na−ND_3 structural model employed was incorrect.

On the other hand, it is obvious from the satisfactory refinement of the synchrotron X-ray data that there is the correct electronic density in the vicinity of the Na and ND_3 positions. Noticing that it is not possible to distinguish between a Na^+ ion (10 electrons) and a ND_3 molecule (10 electrons) by X-ray diffraction, it seems reasonable to explore alternative models by exchanging the Na and ND_3 positions. A new refinement procedure was thus initiated with the Na^+ ions placed in the original X-ray Ne 32*f* (*y*,*y*,*y*; $y \approx 0.583$) positions and the N atoms placed in the original X-ray Na 32*f* (*x*,*x*,*x*; $x \approx 0.484$) positions. The D atoms were now placed in the 96*k* (*x*,*x*,*z*; $x \approx 0.495$, $z \approx 0.415$) sites. In this new model, the geometry of the Na−ND_3 pairs is such that the Na^+ ions are disordered over the corners of the external, while the N atoms of the internal cube (Figure 2b). Every Na^+ ion coordinates with a N at the opposite corner of the internal cube and the ND_3 molecules

adopt their standard geometry. By this simple exchange of positions, the agreement factor for the refinement of the neutron data improved tremendously (R_{wp} = 5.0%) (Figure 3b), while the quality of the refinement of the synchrotron X-ray data was not influenced much by the change in model. Despite the larger displacement of the Na from the center of the octahedral void (~2.0 Å), all the Na−C distances were in the range of 2.8−3.0 Å, showing the absence of sterical crowding.

Because of the good quality of both the X-ray and neutron data, it was possible to explore further the new arrangement of the Na−ND_3 pair by refining the Na and N positions. The refinement proved extremely stable and converged to a value for the Na−N distance of 2.48(2) Å, in good agreement with the typical values found in other Na−NH_3 complexes.[16] Subsequently, the positional parameters of the D atom were refined by using the soft constraint routine of the GSAS program. Within this option, the ND_3 molecule was constrained to its standard gas-phase geometry with weight factors for both angles and bond lengths set to unity to reduce the effect of each restraint component to the minimization function. The refined N and D positions resulted in physically reasonable ND_3 geometries with N−D distances of 0.998(1) Å and D−N−D angles of 109.11(7)°.

Once we determined the location and geometry of the Na−ND_3 pairs, a further series of Rietveld refinements was employed in an attempt to define the exact composition of the KRb(1) sample. After fixing the K and Rb content according to the nominal stoichiometry, the Na, N, and D fractional occupancies were set to be in a 1:1:3 ratio and then were allowed to vary. A slight deficiency in the ammonia content with x = 0.968(8) was identified. Two different models were then tested for the position of the remaining $(1 - x)$ Na cations, which were placed in either the tetrahedral or the octahedral void. In contrast with the earlier X-ray results,[14] the refinement proved to be more stable when the remaining Na cation was residing in the octahedral hole. The Rb^+ ions were also disordered between the tetrahedral and the octahedral sites with occupancies y and $(1 - y)$, respectively. The refinements showed that 6.5(3)% of the Rb^+ ions reside in the center of the octahedral void. The stability of the combined Rietveld refinement of the diffraction profiles was not affected even when the C_{60} positional parameters were varied unconstrained. The three nonequivalent C atoms are at similar distances from the center of the molecule ($R_{C(1)}$= 3.545(4) Å, $R_{C(2)}$= 3.555(2) Å, $R_{C(3)}$= 3.536(2) Å), implying that the C_{60}^{3-} cage is well described as an undistorted sphere of radius R = 3.545(2) Å. This may be compared with the radii of the fullerene cages in neutral C_{60} (3.542 Å), K_3C_{60} (3.552(9) Å), and K_6C_{60} (3.560(8) Å).[17] The mean lengths of the 6:6 and 6:5 bonds at the hexagon−hexagon and hexagon−pentagon junctions are 1.403(3) and 1.447(3) Å, respectively, compared with 1.400(4) and 1.452(13) Å in K_3C_{60}.

After optimization of both the Na−ND_3 and C_{60} geometry and the ND_3 content, the neutron diffraction profile was described perfectly, while the agreement of the calculated profile with the measured X-ray data was not completely satisfactory with some intensity missing for the (111) and (220) cubic reflections. The low 2θ region of the X-ray diffraction profile is very sensitive to the cation composition. For this reason, a final series of combined Rietveld refinements was performed in which the fractional occupancies of Na, K, and Rb were refined independently without any constraint (the constrained 1:1:3 ratio on the Na(pseudo-octahedral), N, and D fractional occupancies was retained). Because of the several refined parameters and correlations between the occupation numbers of the ions in the octahedral void and the ND_3 geometry, the weight factors of the soft constraint on the D−N−D angles and N−D bond lengths were now increased to 100. As a result, the agreement factor of the X-ray diffraction profile improved from R_{wp} = 5.1% to R_{wp} = 4.7%. The results of the final combined refinement on the KRb(1) sample are shown in Figure 4 (combined agreement factors: R_{wp} = 4.6%, R_{exp} = 6.6%; a = 14.3358(2) Å) with the fitted parameters summarized in Table 1. A schematic diagram of the crystal structure is shown in Figure 5. Compared to the earlier refinements, the major change has been the presence of a deficiency in the K content (0.85-(1)), while the ND_3 geometry and occupancy together with the C_{60}^{3-} cage geometry were not affected. Finally, a detailed inspection of N−C and D−C distances showed the absence of short N−C contacts (>3.476(6) Å) but revealed some unusually close D−C contacts of 2.555(6) and 2.590(4) Å (Table 2).

The synchrotron X-ray and neutron powder diffraction profiles collected at 10 K on the KRb(2) sample were also analyzed by a combined Rietveld refinement. At the beginning, the KRb(1) structural model was employed and a series of refinements were then started following the procedure already described. The fractional occupancies of the Rb(tetrahedral), Rb(octahedral), and K ions were initially fixed to the values obtained for KRb(1). The refinements proceeded smoothly with no significant changes either in the C_{60}^{3-} cage or in the Na−ND_3 pair geometry. As expected, the ammonia content refined to a smaller value (x = 0.792(8)) compared to that in KRb(1) with subsequent increase of the concentration of the remaining Na cation in the octahedral void. Again, some problems were encountered with the calculated intensities of the X-ray diffraction profile for the (111) and (220) cubic reflections (R_{wp} = 7.6%). The three KRb samples in the present work were synthesized starting from different reactant batches that were annealed at different temperatures. This means that some variation from sample to sample in the stoichiometric composition is not precluded. For this reason, the cation fractional occupancies were allowed to vary independently without constraints in the final refinement cycles. We only retained the constraint on the ratio of the Na(pseudo-octahedral), N, and D fractional occupancies to 1:1:3 with a weight factor set equal to 100. As a result, the X-ray agreement factor improved to R_{wp} = 5.0%. The results of the final combined refinement on the KRb(2) sample and selected distances and angles are summarized in Figure 1S and Tables 1S and 2S (combined agreement factors: R_{wp} = 4.7%, R_{exp} = 4.1%; a = 14.3256(2) Å). Exactly the same approach was used to refine the synchrotron X-ray and neutron powder diffraction profiles collected at 10 K on the KRb(3) sample. The final refinement and the fitted parameters and selected distances and angles are shown in Figure 2S and Tables 3S and 4S (combined agreement factors: R_{wp} = 5.3%, R_{exp} = 4.3%; a = 14.3244(2) Å). The ammonia content decreased further (x = 0.72(4)), while no changes are observed in the geometry of either the C_{60}^{3-} cage or the Na−

(16) Fowkes, A. J.; Fox, J. M.; Henry, P. F.; Heyes, S. J.; Rosseinsky, M. J. *J. Am. Chem. Soc.* **1997**, *119*, 10413.
(17) Allen, K. M.; David, W. I. F.; Fox, J. M.; Ibberson, R. M.; Rosseinsky, M. J. *Chem. Mater.* **1995**, *7*, 764.

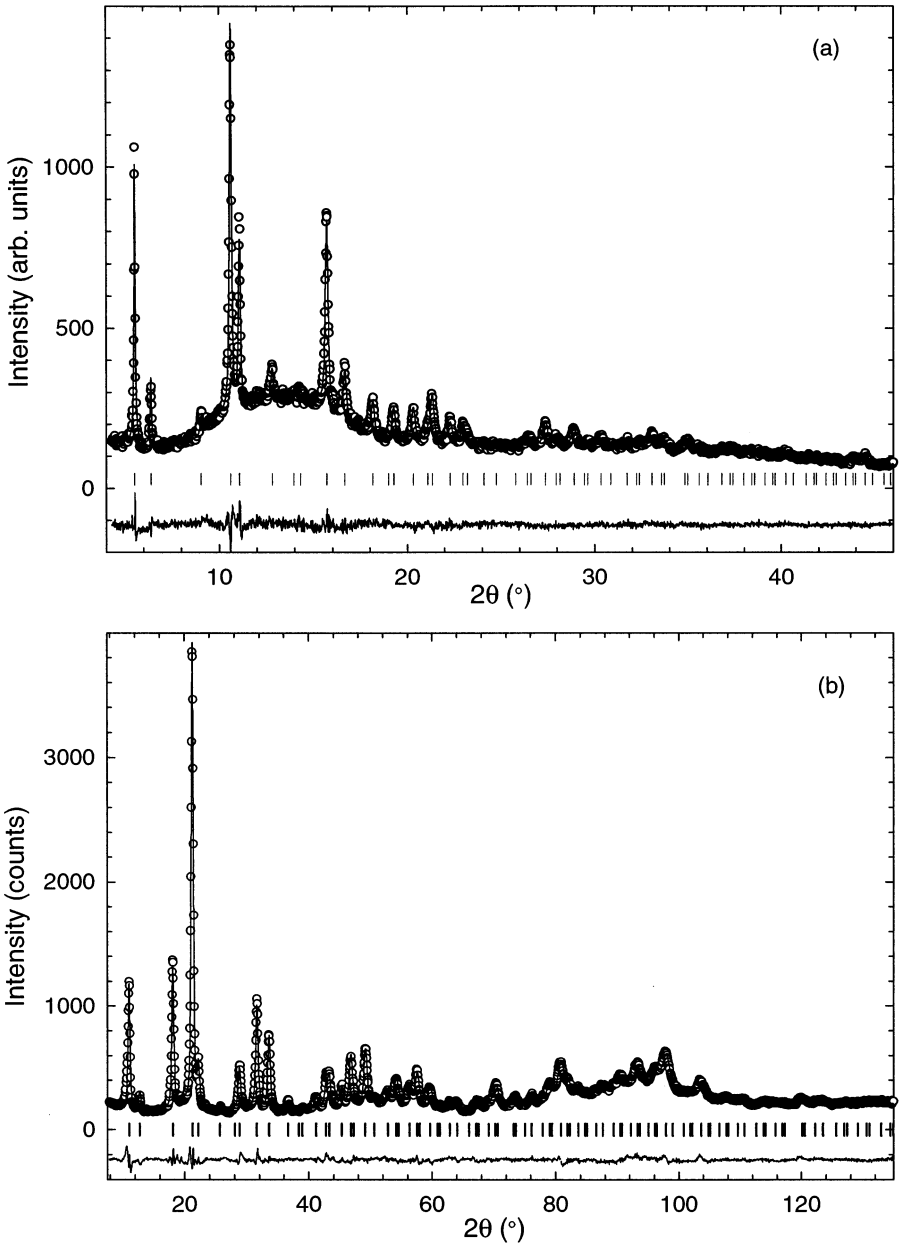

Figure 4. Final observed (o) and calculated (solid line) powder (a) synchrotron X-ray ($\lambda = 0.80002$ Å) and (b) neutron ($\lambda = 1.5944$ Å) diffraction profiles for $(ND_3)_{0.97}NaKRbC_{60}$ (KRb(1)) at 10 K. In each case, the lower solid line shows the difference profile and the tic marks show the reflection positions.

Table 1. Refined Parameters for $(ND_3)_{0.97}NaKRbC_{60}$ (KRb(1)) at 10 K in the Space Group $Fm\bar{3}m$ with a Unit Cell Parameter, $a =$ 14.3358(2) Å ($R_{wp} = 4.6\%$, $R_{Exp} = 6.6\%$)

atom	site	*x*	*y*	*z*	B_{iso}/Å^2	*n*
C(1)	96*j*	0	0.0483(2)	0.2425(2)	0.66(4)	0.5
C(2)	192*l*	0.2121(1)	0.0814(2)	0.0995(2)	0.66(4)	0.5
C(3)	192*l*	0.1806(2)	0.1603(2)	0.0503(1)	0.66(4)	0.5
Rb_T	8*c*	0.25	0.25	0.25	1.11(7)	0.466(2)
K	8*c*	0.25	0.25	0.25	1.11(7)	0.426(7)
Na_{pO}	32*f*	0.582(1)	0.582(1)	0.582(1)	4.9(2)	0.121(1)
N	32*f*	0.4824(3)	0.4824(3)	0.4824(3)	4.9(2)	0.121(1)
D	96*k*	0.4955(3)	0.4152(3)	0.4955(3)	11.1(5)	0.121(1)
Na_O	4*b*	0.5	0.5	0.5	4.9(2)	0.017(3)
Rb_O	4*b*	0.5	0.5	0.5	4.9(2)	0.065(3)

ND_3 pair. From these results, it is clear that as the annealing temperature of the $(ND_3)_xNaKRbC_{60}$ samples increases, the ammonia concentration *x* decreases monotonically and is accompanied by a decrease in the cubic lattice constant *a*. At the same time, the cation fractional occupancy in the center of the octahedral void increases. The changing value of *x* does not influence the Na−ND_3 pair geometry for which the Na−N distance remains essentially constant at ∼2.48 Å. In all cases, short D−C contacts in the range 2.5−2.6 Å are present (Table 3).

Structural Analysis of the $(ND_3)_xNaRb_2C_{60}$ Series. The synchrotron X-ray and neutron diffraction data collected at 10 K on the three samples of the $(ND_3)_xNaRb_2C_{60}$ series were also analyzed following the procedure used for $(ND_3)_xNaKRbC_{60}$. A combined Rietveld refinement was performed on the Rb2(2) sample employing the same structural model already described for KRb(1) with the Rb^+ cations disordered over the tetrahedral and octahededral sites. The results of the final combined refinement on the Rb2(2) sample are shown in Figure 6 (combined agreement factors: $R_{wp} = 4.7\%$, $R_{exp} = 4.8\%$; $a =$ 14.42598(8) Å) with the fitted parameters and selected bond

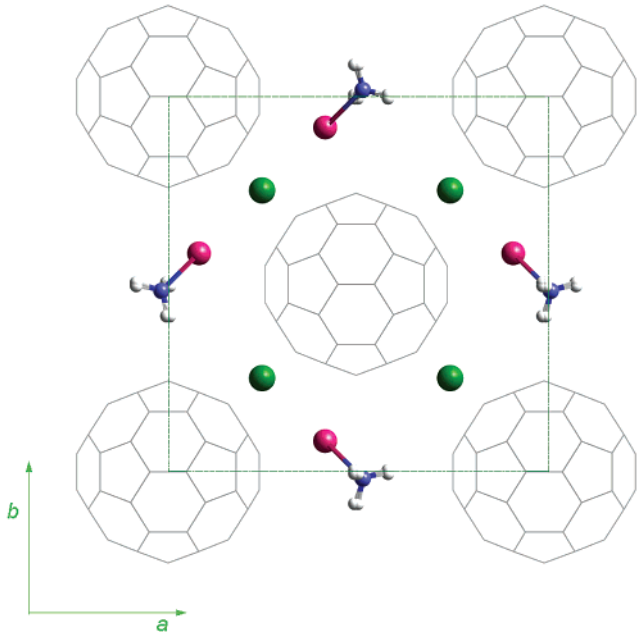

Figure 5. Basal-plane projection of the structure of the $(ND_3)_xNaA_2C_{60}$ family. The C_{60} units are merohedrally disordered, while the disorder of the $Na-ND_3$ pairs is as in Figure 2b (only one of the eight possible orientations is shown here for clarity). The dotted lines show the size of the unit cell.

Table 2. Selected Distances (Å) and Angles (deg) in $(ND_3)_{0.97}NaKRbC_{60}$ (KRb(1)) at 10 K

C(1)−C(1) (6:6 bonds) (×6)	1.386(5)
C(2)−C(3) (6:6 bonds) (×24)	1.407(3)
C(1)−C(2) (6:5 bonds) (×24)	1.445(2)
C(3)−C(3) (6:5 bonds) (×12)	1.443(3)
C(2)−C(3) (6:5 bonds) (×24)	1.451(3)
Na_{pO}−N (×1)	2.48(2)
N−D (×3)	0.9990(6)
D−N−D (×3)	109.139(7)
D−C(1) (×3)	2.555(6)
D−C(1) (×3)	2.590(4)
Na−C(1) (×6)	2.817(6)

distances and angles listed in Tables 5S and 6S. Both the C_{60}^{3-} and the $Na-ND_3$ pair geometry change little between the two series. By using the soft constraint option within the GSAS program with a weight factor of 100, the Na−N and N−D distances refined to values of 2.480(1) Å and 1.000(1) Å, respectively. The N−D−N angle is 109.14(1)° and the Na displacement from the center of the octahedral void is 2.145(6) Å. The refined structure did not show any unusual Na−C interaction (larger than 2.8 Å) but again short D−C contacts (~2.64 Å) are evident as before. The three nonequivalent C atoms describe the C_{60}^{3-} cage ($R_{C(1)}$ = 3.585(2) Å, $R_{C(2)}$ = 3.555(1) Å, $R_{C(3)}$ = 3.542(1) Å) as a sphere of radius R = 3.556(1) Å. The mean lengths of the 6:6 and 6:5 bonds at the hexagon−hexagon and hexagon−pentagon junctions are 1.416(2) Å and 1.446(2) Å, respectively. The refined composition showed a deficiency in ammonia content, x = 0.856(8).

A combined refinement was also performed on the synchrotron X-ray and neutron diffraction data collected on the Rb(1) sample. Because of the inferior quality of the data, it was not possible to refine the fullerene unit geometry, and only the parameters relating to the $Na-ND_3$ geometry and cation composition and ND_3 content were varied. The refinement proceeded smoothly and the results are shown in Figure 3S and in Tables 7S and 8S (combined agreement factors: R_{wp} = 6.0%, R_{exp} = 3.9%; a = 14.4285(4) Å; ammonia content, x = 0.920(8)). Only synchrotron X-ray data were collected for the Rb(3) sample, which was of poorer quality. During the refinement, only the parameters relating to the cation and ammonia composition were varied (Tables 9S and 10S) and the ammonia content was refined to x = 0.79(2). The resulting refinement is shown in Figure 4S (agreement factors: R_{wp} = 9.6%, R_{exp} = 4.7%; a = 14.3879(2) Å).

In agreement with what was observed for the $(ND_3)_x$-$NaKRbC_{60}$ series, the results obtained for the three $(ND_3)_x$-$NaRb_2C_{60}$ samples show that the decrease in ammonia concentration x with annealing temperature is accompanied by a reduction in the size of the cubic unit cell and an increase in the cation fractional occupancy of the center of the octahedral void (Table 4). Short D−C contacts in the range 2.6−2.7 Å are again present. On the other hand, the decrease in x does not affect geometry of the $Na-ND_3$ pairs which display a Na−N distance of ~2.48 Å.

Discussion

Intercalated fullerides display rich structural and electronic properties, which are sensitively controlled by several factors. The conventional metallic A_3C_{60} (A = alkali metal) systems adopt cubic structures with their conduction band derived from the LUMO t_{1u} levels of C_{60} and superconductivity restricted only close to half filling.[5,6] There is a strong correlation between the appearance of superconductivity and the interfullerene separation, the orientational order/disorder of the fullerene units, the valence state of C_{60}, the orbital degeneracy of the LUMO states, the existence of low-symmetry distortions, and the strength of the alkali-C_{60} interactions.[18] We will consider some of these factors in turn in our attempt to rationalize the unusual properties of the $(ND_3)_xNaA_2C_{60}$ systems, drawing from our detailed structural results.

The superconducting properties of the $(NH_3)_xNaA_2C_{60}$ ($0.7 \leq x \leq 1$, A = K, Rb) series are unusual and, in view of the highly complex structural chemistry revealed by the present work, are not straightforward to rationalize. Empirically, the superconducting transition temperature T_c increases with increasing sample annealing temperature T_{ann}. Although the latter does not affect the cubic crystal symmetry, it leads to well-defined changes in the sample stoichiometry (principally a decrease in ammonia content x) and in the size of the unit cell (a decrease in interfullerene separation). However, the present structural study reveals several subtle structural features, which should also affect sensitively the electronic properties of the systems. In the $(ND_3)_xNaKRbC_{60}$ series, T_c increases only slighlty with T_{ann} and all three samples show a broad transition which could imply the existence of phase inhomogeneities, the presence of impurities, or the development of distinct inter- and intragrain contributions to the shielding currents in the granular samples.[3] The collected diffraction profiles did not show additional peaks which could be attributed to impurities. On the other hand, the difference in size between the K^+ and Rb^+ cations, which are both disordered in the tetrahedral voids, could lead to local phase inhomogeneities and regions, which could be regarded as solid solutions of $(ND_3)_xNaK_2C_{60}$ and $(ND_3)_x$-$NaRb_2C_{60}$ compositions, thereby affecting the superconducting

(18) Margadonna, S.; Prassides, K. *J. Solid State Chem.*, in press.

Table 3. Selected Data for the $(ND_3)_xNaKRbC_{60}$ Series at 10 K

	$(ND_3)_{0.97}NaKRbC_{60}$	$(ND_3)_{0.79}NaKRbC_{60}$	$(ND_3)_{0.72}NaKRbC_{60}$
a (Å)	14.3358(2)	14.3256(2)	14.3244(2)
$n(Na_{pO})$	0.121(1)	0.099(1)	0.090(1)
$n(Na_O)$	0.017(3)	0.191(3)	0.288(6)
$n(Rb_O)$	0.065(3)	0.153(3)	0.145(2)
$n(Rb_T)$	0.466(2)	0.437(1)	0.423(3)
$n(K_T)$	0.426(7)	0.454(6)	0.451(8)
total ammonia content, x	0.968(8)	0.792(8)	0.72(4)
total Rb content	0.997(7)	1.027(5)	0.99(5)
total K content	0.85(1)	0.91(1)	0.90(2)
total Na content	0.99(1)	0.98(1)	1.01(1)
total cation content	2.84(3)	2.92(3)	2.90(4)
Na-displacement (Å)	2.050(2)	2.031(3)	2.030(8)
N-displacement (Å)	0.438(8)	0.448(3)	0.450(8)
C(1)−D contacts (Å)	2.555(6); 2.590(4)	2.515(10); 2.553(6)	2.513(6); 2.553(4)
R_{wp}; R_I (neutrons)	4.6; 3.1%	4.5; 3.2%	4.4; 2.8%
R_{wp}; R_I (X-rays)	4.7; 4.0%	5.0; 4.7%	6.5; 5.1%
T_c (K)	12	13.5	14.5

properties. The onset of superconductivity is more sharply defined for the $(ND_3)_xNaRb_2C_{60}$ series and T_c increases by ∼3 K on increasing the annealing temperature to 100 °C. With further increase of T_{ann} to 120 °C, T_c increases by ∼6 K and a rather broad transition is observed. The synchrotron X-ray diffraction profile collected on the Rb2(3) sample confirms the presence of some unindexed peaks which are attributed to impurities.

The structural chemistry of A_3C_{60} fullerides strongly depends on the difference in size between the metal ions and the octahedral and tetrahedral interstices in the unit cell. The size of the octahedral void is large enough to accommodate all alkali ions, while the tetrahedral one has a size larger than Na^+ but smaller than K^+. The fact that NaA_2C_{60} (A = K, Rb) cannot be synthesized can be understood in terms of the energetically unfavorable situation to accommodate Na^+ and K^+/Rb^+ in the same tetrahedral sites. Upon ammoniation, however, single phases of $(ND_3)_xNaA_2C_{60}$ are stabilized. The large $Na-ND_3$ units of the disordered $[Na_8(ND_3)_8]_{1/8}$ clusters are now accommodated in the octahedral holes with the K^+/Rb^+ ions residing in the tetrahedral sites. This leads to steric hindrance, which favors the adoption of an fcc structure (space group $Fm\bar{3}m$) comprising merohedrally disordered C_{60} units. The resulting interfullerene separation is on the order of ∼10.14−10.20 Å at 10 K, comparable to those observed in the Rb_3C_{60} and Rb_2CsC_{60} superconductors (T_c = 29 and 31 K). Like the latter fullerides, the $(NH_3)_xNaA_2C_{60}$ ($0.7 \le x \le 1$, A = K, Rb) series does not also show any orientational ordering transition with decreasing temperature.

The structure of the $(ND_3)_xNaA_2C_{60}$ ($0.7 \le x \le 1$, A = K, Rb) compounds was refined sufficiently well to allow a detailed discussion of the plethora of interatomic and intermolecular interactions. Despite the apparent overall simplicity and cubic symmetry (Figure 5), it is characterized by remarkable degrees of orientational disorder of both the sodium ammonia and the C_{60} units. First coordination of ND_3 to Na^+ is strong with a Na−N bond distance of 2.48 Å. The refined geometry of ammonia is quite similar to that in the gas phase with N−D bond lengths of 1.0 Å. The D−N−D angle has increased somewhat to 109°. This is expected, as the bonding interaction between N and Na^+ should result in an opening of the D−N−D angle. Each Na^+ and N atom are shifted toward three of the six neighboring C_{60} units (Figure 7a) as they are displaced from the center of the octahedral interstices by ∼2.0 Å and ∼0.5 Å, respectively. The resulting six shortest Na−C distances are ∼2.8 Å (Tables2 and 6S), comparable to those in Na_2CsC_{60}[19] and larger than the sum of the ionic radius of Na^+ and the van der Waals radius of C, implying the absence of strong Na−C interactions and partial charge transfer to C_{60}. On the other hand, the nonbonded contacts between each D atom of ND_3 and the two nearest C atoms of neighboring C_{60} (Figure 7a) are in the range of 2.51−2.67 Å (Tables 3 and 4), considerably shorter than both the sum of the carbon and deuterium van der Waals radii and the closest intermolecular carbon−hydrogen contacts in solid benzene (2.95 Å).[20] Figure 7b shows the mode of coordination of a single C_{60} unit through six of its hexagon−hexagon fusions to appropriately oriented D atoms of six neighboring octahedrally disposed ND_3 molecules. As the 6:6 bonds of C_{60} are electron rich, the structural results strongly suggest the existence of a network of weak N−D···π(6:6) hydrogen bonding prevailing throughout the structure.

Optimization of this hydrogen-bonding structural motif should be responsible for the stabilization of the highly disordered cubic structure observed in $(ND_3)_xNaA_2C_{60}$. An ordered asymmetric $(ND_3)Na^+$ unit in the octahedral holes allows a maximum of only three N−D···π(6:6) hydrogen bonds to form, the remaining three C_{60}'s coordinating to Na^+ (Figure 8). Such an arrangement repeated in three dimensions should lead to a reduction in symmetry as it has been observed in the larger $(ND_3)K^+$ unit which orders antiferroelectrically in orthorhombic $(ND_3)K_3C_{60}$.[9] Evidently in the present compounds, disorder of the $(ND_3)Na^+$ units about the diagonals of the two interpenetrating $[Na_8(ND_3)_8]_{1/8}$ cubes allows every C_{60} molecule in the structure to have an identical coordination environment and to sample the maximum number of N−D···π(6:6) bonding interactions, while retaining cubic symmetry.

Another point arising from the results of the present refinement that is of particular interest is the monotonic decrease in lattice dimensions, a, accompanying the gradual loss of ammonia with increasing annealing temperature. Across the $(ND_3)_xNaKRbC_{60}$ series, x decreases from 0.97 to 0.72 and the lattice contracts by 0.080(3)%, while across the $(ND_3)_xNaRb_2C_{60}$ series, x decreases from 0.92 to 0.79 and the lattice contracts by 0.282-

(19) Prassides, K.; Christides, C.; Thomas, I. M.; Mizuki, J.; Tanigaki, K.; Hirosawa, I.; Ebbesen, T. W. *Science* **1994**, *263*, 950.
(20) Desiraju, G. R.; Gavezzotti, A. *Acta Crystallogr., Sect. B* **1989**, *45*, 473.

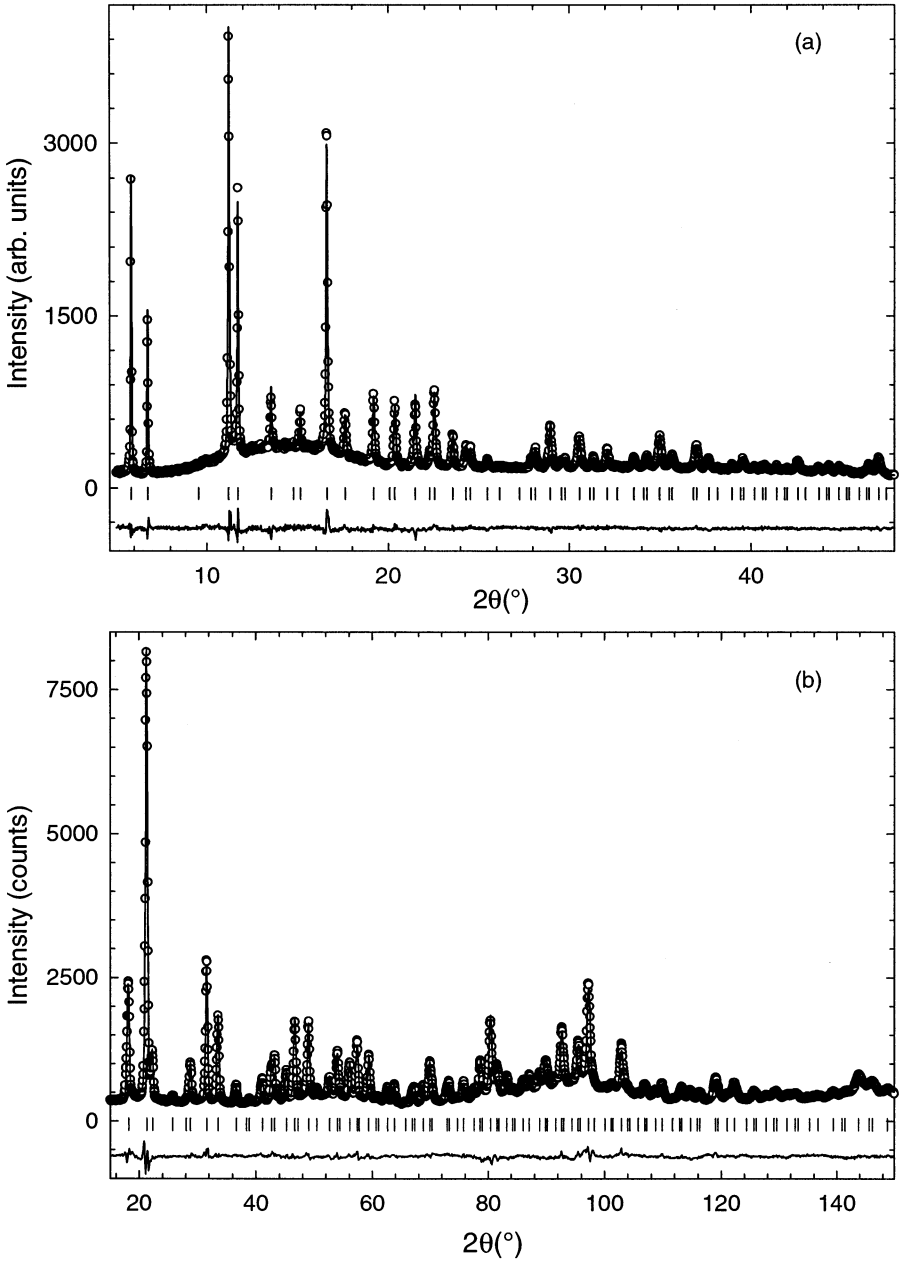

Figure 6. Final observed (o) and calculated (solid line) powder (a) synchrotron X-ray ($\lambda = 0.85041$ Å) and (b) neutron ($\lambda = 1.5944$ Å) diffraction profiles for $(ND_3)_{0.86}NaRb_2C_{60}$ (Rb(2)) at 10 K. In each case, the lower solid line shows the difference profile and the tic marks show the reflection positions.

(4)%. As the geometry of the $(ND_3)Na^+$ units and the displacements of Na^+ and ND_3 from the center of the octahedral holes are virtually unaffected across the series, the resulting lattice contraction should be related to the partial occupation of the octahedral sites by the uncoordinated Na^+ and Rb^+ ions. The amount of uncoordinated cations increases with increasing ammonia loss and because of their smaller size compared to the $[Na_x(ND_3)_x]$ cluster, this would result in smaller lattice dimensions.

Returning to the discussion of the superconducting properties of the $(NH_3)_xNaA_2C_{60}$ ($0.7 \leq x \leq 1$, A = K, Rb) compounds, their behavior appears to defy the universal relationship between T_c and interfullerene separation, and their T_c's (and density of states at the Fermi level, $N(\epsilon_F)$[21]) are dramatically lower when compared with other isostructural fullerides (e.g., Rb_2CsC_{60}) with comparable C_{60}–C_{60} contacts. In addition, the trend is even inverted and the T_c values increase with decreasing cubic lattice dimensions. We recall that the electronic properties of alkali fullerides are those of highly correlated metals and a transition to a Mott−Hubbard insulating state is expected for small enough conduction bandwidths at large interfullerene spacings.[22] This has been realized in $(NH_3)K_3C_{60}$ where a combination of crystal symmetry lowering, which lifts the degeneracy of the t_{1u} orbitals, and increased C_{60}–C_{60} separation, which reduces the bandwidth, results in an antiferromagnetic Mott insulating ground state.[10] In addition, when the metal−insulator boundary is approached from the metal side, the screening of the interelectronic repulsions in the conduction band becomes increasingly inefficient and the rapidly increasing electron correlation effects

(21) Tou, H.; Muroga, N.; Maniwa, Y.; Shimoda, H.; Iwasa, Y.; Mitani, T. *Physica B* **2000**, *281*, 1018.

(22) Koch, E.; Gunnarsson, O.; Martin, R. M. *Phys. Rev. Lett.* **1999**, *83*, 620.

Table 4. Selected Data for the $(ND_3)_xNaRb_2C_{60}$ Series at 10 K

	$(ND_3)_{0.92}NaRb_2C_{60}$	$(ND_3)_{0.86}NaRb_2C_{60}$	$(ND_3)_{0.79}NaRb_2C_{60}$
a (Å)	14.4285(4)	14.42598(8)	14.3879(2)
$n(Na_{pO})$	0.115(1)	0.107(1)	0.099(3)
$n(Na_O)$	0.027(5)	0.072(5)	0.224(2)
$n(Rb_O)$	0.093(5)	0.101(2)	0.223(2)
$n(Rb_T)$	0.850(2)	0.867(2)	0.896(1)
total ammonia content, *x*	0.920(8)	0.856(8)	0.79(2)
total Rb content	1.793(9)	1.835(6)	2.015(4)
total Na content	0.947(1)	0.928(1)	1.02(3)
total cation content	2.74(2)	2.84(2)	3.04(3)
Na-displacement (Å)	2.19(2)	2.145(6)	2.07(2)
N-displacement (Å)	0.29(2)	0.335(6)	0.41(2)
C(1)−D contacts (Å)	2.669(9); 2.68(2)	2.635(5); 2.638(3)	
R_{wp}; R_I (neutrons)	5.6; 3.1%	4.5; 2.9%	
R_{wp}; R_I (X-rays)	6.9; 4.3%	5.1; 3.8%	9.3; 5.3%
T_c (K)	6	9	15

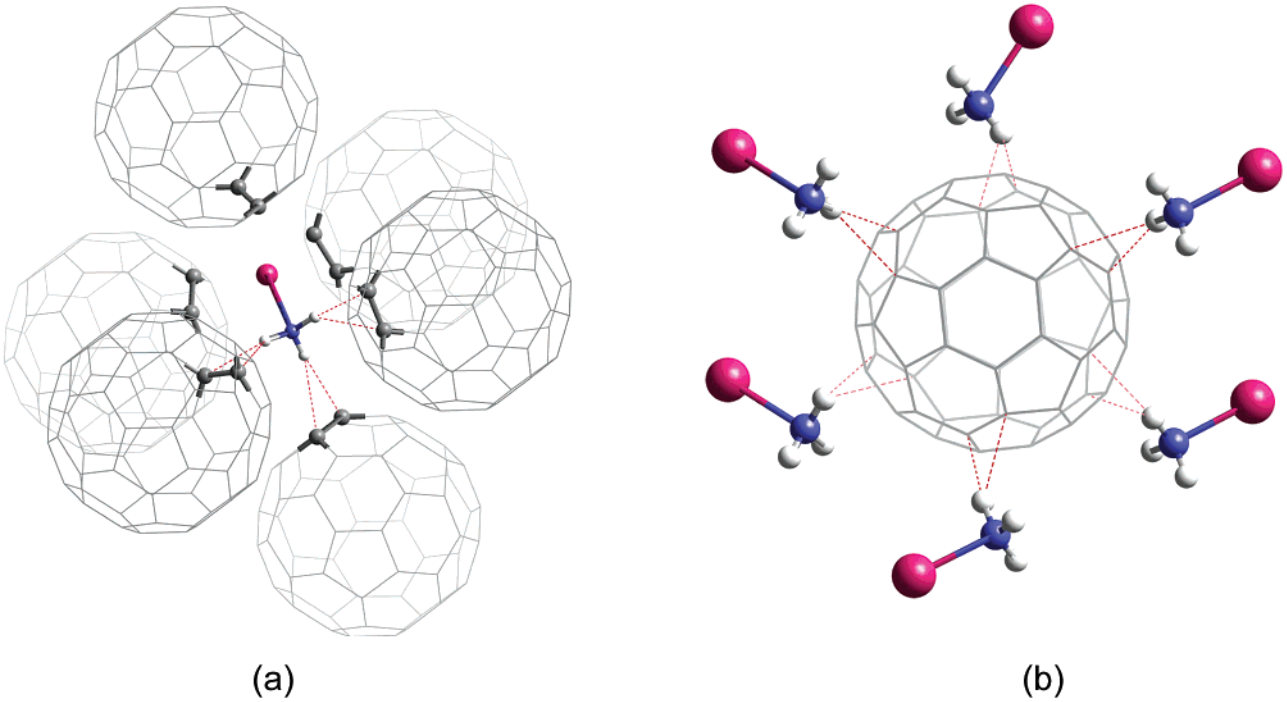

Figure 7. (a) Coordination environment of a $Na(ND_3)^+$ pair in the octahedral holes of the $(NH_3)_xNaA_2C_{60}$ crystal structure. Only one of the possible eight orientations is shown for clarity. (b) Coordination environment of the C_{60}^{3-} units for the maximum number of N−D···π(6:6) hydrogen bonds possible.

could lead to a reduction in T_c, as observed in $Rb_{2-x}Cs_{1+x}C_{60}$ fullerides.[3] However, the range of lattice dimensions encountered in cubic $(ND_3)_xNaA_2C_{60}$ does not approach the critical interfullerene separations necessary for sufficient band narrowing to occur and for superconductivity to be suppressed because of strong electron correlation effects.

Earlier work[14] stressed the potential importance of the large off-centering of the Na^+ ion (~2.0 Å) which could have a detrimental effect on superconductivity as C_{60} should experience a noncubic Coulomb potential causing the lifting of the triple degeneracy of the t_{1u} levels and suppressing the pairing mechanism in analogy with $(NH_3)K_3C_{60}$. However, the Na−ND_3 pairs in $(ND_3)_xNaA_2C_{60}$ are statically disordered about the diagonals of two concentric cubes and space averaging leads to maintaining the overall cubic crystal symmetry and thereby reducing the importance of such distortion effects. In addition, to explain the increase in T_c with decreasing ammonia content, an accompanying relaxation of the Na^+ displacement from the center of the octahedral hole is required but this is not observed experimentally (Tables 3 and 4). Moreover, the effect of applied pressure on T_c differs from that of chemical pressure and the "universal" behavior is recovered as T_c decreases with decreasing interfullerene separation[23] despite the retention of off-centered Na^+ ions. It may be possible, however, that the increase in the occupation of the octahedral hole by uncoordinated ions, which accompanies decreasing ammonia content, could lead to reduction of the local noncubic crystal fields. The total cation content derived from the present refinements (Tables 3 and 4) is invariably smaller than 3 implying the existence of some cation nonstoichiometry which could lead to deviations from half filling of the conduction band and suppressed T_c's.[5,6]

However, our structural results point to a more straightforward ammonia-specific origin of the observed nonrigid band behavior in the $(ND_3)_xNaA_2C_{60}$ systems. The structure is controlled by a network of hydrogen-bonding N−D···π(6:6) interactions between the $Na(ND_3)^+$ and C_{60}^{3-} units which sensitively affects

(23) Takenobu, T.; Shimoda, H.; Iwasa, Y.; Mitani, T.; Kosaka, M.; Tanigaki, K.; Brown, C. M.; Prassides, K. *Mol. Cryst. Liq. Cryst.* **2000**, *340*, 599.

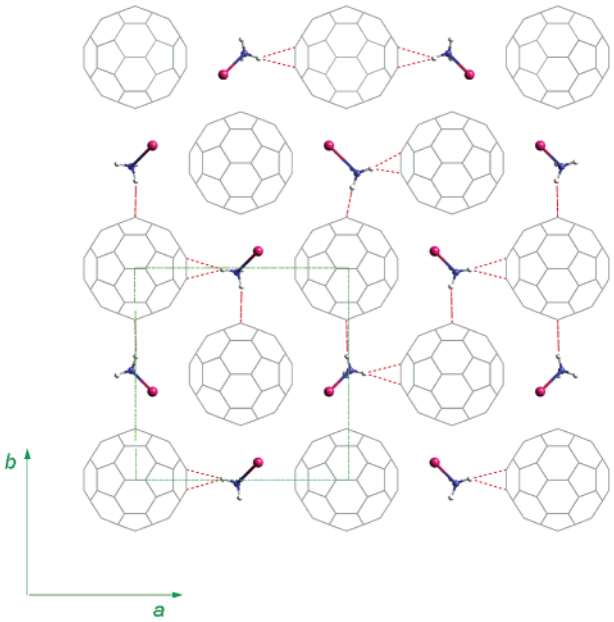

Figure 8. Basal-plane projection of the structure of the $(NH_3)_xNaA_2C_{60}$ series showing the network of hydrogen bonding N−D···π(6:6) interactions between the $Na(ND_3)^+$ and C_{60}^{3-} units (only one of the eight possible orientations of $Na(ND_3)^+$ is shown).

electron hopping between neighboring fullerene molecules and the electronic states near the Fermi level. As this structural motif is progressively disrupted by the partial loss of ND_3 molecules, the shape of the conduction band and the electronic properties resemble more those of the conventional t_{1u} superconductors and T_c rises toward the values expected from the "universal" relationship for the appropriate interfullerene separations. Such an ammonia-specific influence of the electronic properties is also consistent with the high-pressure results as physical pressure does not alter the hydrogen-bonding network and only affects the size of the conduction bandwidth, thereby leading to reduced T_c upon contraction.

Conclusions

Ambient temperature co-intercalation of ammonia and alkali metals (K, Rb) in C_{60} yields the superconducting salts, $(ND_3)_x$-$NaKRbC_{60}$ and $(ND_3)_xNaRb_2C_{60}$ ($x \sim 1$). Cubic crystal symmetry is retained and the expanded fcc structures adopted comprise merohedrally disordered C_{60}^{3-} ions and Na^+-ND_3 pairs residing in the octahedral holes. The latter are disordered about the diagonals of two "interpenetrating" cubes with Na^+ and ND_3 displaced from the center of the hole by ~2.0 Å and ~0.5 Å, respectively. This results in a novel supramolecular architecture in which each D atom of every ND_3 molecule is involved in weak hydrogen-bonding interactions with an electron rich 6:6 C−C bond of a neighboring fulleride ion, giving rise to a three-dimensional network of intermolecular interactions. The optimal octahedral nesting of six D atoms over six 6:6 bonds of C_{60} units is presumably responsible for the highly disordered structure adopted and the absence of a symmetry-lowering distortion. In addition, the presence of the N−D···π(6:6) bonding interactions should modify the electronic states of C_{60} through orbital mixing, suppress electron hopping between neighboring fulleride ions, and lead to an increased conduction bandwidth. Therefore, it provides a plausible explanation for the unusual highly diminished values of the superconducting transition temperatures T_c when compared with other isostructural alkali fullerides (Rb_3C_{60}, Rb_2CsC_{60}) at the same interfulleride separations. Mild heating of both $(ND_3)_xNaKRbC_{60}$ and $(ND_3)_xNaRb_2C_{60}$ leads to a progressive partial loss of ND_3 molecules. This has as a consequence the disruption of the ND_3–C_{60} intermolecular interactions as the octahedral holes are now increasingly occupied by uncoordinated ions, which also reduce the local noncubic crystal fields, and leads to an increase in T_c despite the accompanying gradual lattice contraction. The present family of ammoniated alkali fullerides provides an excellent example of the potential richness of the structural properties of fulleride salts and demonstrates the extreme sensitivity of their electronic properties even to weak intermolecular interactions.

Acknowledgment. We thank the NEDO Frontier Carbon Technology program and the Royal Society for financial support, Jesus College (Cambridge) for a Research Fellowship to S.M., the ESRF and Spring-8 for provision of synchrotron X-ray beamtime, and the ILL for neutron beamtime. We thank A. N. Fitch (ESRF), T. Hansen (ILL), I. Margiolaki (University of Sussex), E. Nishibori, and M. Takata (Nagoya University) for help with the experiments.

Supporting Information Available: Figures of all additional Rietveld refinements of the neutron and synchrotron X-ray diffraction data, and tables of the refinement parameters and selected distances and angles (PDF). This material is available free of charge via the Internet at http://pubs.acs.org.

JA026775K